Inorg. Chem. **2002**, *41*, 6867–6874

[*n*.1.1]-(2,6)-Pyridinophanes: A New Ligand Type Imposing Unusual Metal Coordination Geometries

Andrei N. Vedernikov,* John C. Huffman, and Kenneth G. Caulton*

Department of Chemistry and Molecular Structure Center, Indiana University, Bloomington, Indiana 47405-7102

Received June 24, 2002

A series of new ligands with three pyridines linked into a macrocycle by various CH_2, CMe_2, and CH_2CH_2 groups at all sites ortho to the pyridine nitrogen have been synthesized and attached to $PdCl_2$ or $PtMe_2$. The ligands bind to them through only two nitrogens, and the third pyridine is constrained in close proximity to the planar complex with a filled d_{z^2} orbital. Rapid reversible migration of $PdCl_2$ or $PtMe_2$ to the unused pyridine nitrogen is observed at 20 °C in the case of the CH_2-bridged macrocycle and does not occur in the case of the CMe_2-bridged analogue, and the mechanism of this fluxionality has been established by NMR and computational techniques.

Introduction

[*n*.1.1]-(2,6)-Pyridinophanes (*n* = 1, 2, ...), **1**, represent a class of ligands that crowd a number of pyridine donors into compact form. Depending on their rigidity (*n* value), they can serve as a preorganized metal coordination unit. For example, [1.1.1]-(2,6)-pyridinophane, **1** (*n* = 1), has 3-fold symmetry that would appear to force facial tridentate geometry on an attached metal. Tetramethyl-[2.1.1]-(2,6)-pyridinophane, **2**, is more flexible because of the larger ethylene bridge but perhaps less able to bind to a metal because of the four methyl substituents as compared with its nonmethylated analogue **3**. While the first representatives of [1.1.1.1]-(2,6)-pyridinophanes or calyx[4]pyridines have been synthesized only recently, both carbon-[1] and sulfur-bridged [1.1.1]-(2,6)-pyridinophanes are known at the moment.[2,3] The known carbon-bridged [1.1.1]-(2,6)-pyridinophanes bear oxo- or two alkoxy-substituents at bridging carbon atoms, which affect dramatically their coordination behavior.[4] No reports about carbon- or heteroatom-bridged [*n*.1.1]-pyridinophanes with *n* > 1 are available. We report here on attractive synthetic routes to macrocycles **2** and **3** and a study of the outcome of binding of **2** and **3** to $PdCl_2$ and $PtMe_2$, metals whose d^8 electronic configuration would seem to demand a coordination geometry (planar) for which either **2** or **3** is completely unsuited. Learning how the selected molecules accommodate this compromising situation will be seen to reveal the interactions between a metal center with a filled d_{z^2} orbital and a nucleophilic pyridine (lone pair as well as occupied π orbitals).

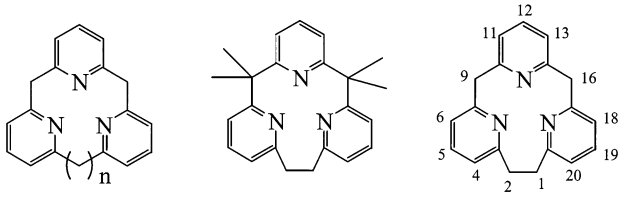

1 **2** **3**

Experimental Section

General. All manipulations were carried out under purified argon using standard Schlenk and glovebox techniques. Solvents were dried and distilled following standard protocols and stored in gastight bulbs under argon. All reagents for which a synthesis is not given are commercially available from Aldrich or Pressure Chemicals and were used as received without further purification. All NMR solvents were dried, vacuum-transferred, and stored in an argon-filled glovebox. 1,2-Bis(2-pyridyl)ethane[5] and tetramethylbis(dimethylsulfide)diplatinum(II)[6] have been synthesized according to the published procedures. ^1H and ^{13}C NMR spectra

* Authors to whom correspondence should be addressed. E-mail: caulton@indiana.edu (K.G.C.); avederni@indiana.edu (A.N.V.). A.N.V. is on leave from the Chemical Faculty, Kazan State University, Kazan, Russia.

(1) Newkome, G. R.; Joo, Y. J.; Theriot, K. J.; Fronczek, F. R. *J. Am. Chem. Soc.* **1986**, *108*, 6074.
(2) Konig, B.; Fonseca, M. H. *Eur. J. Inorg. Chem.* **2000**, 2303.
(3) Reistad, K. R.; Groth, P.; Lie, R.; Undheim, K. *J. Chem. Soc., Chem. Commun.* **1972**, 1059.
(4) Newkome, G. R.; Joo, Y. J.; Evans, D. W.; Fronczek, F. R.; Baker, G. R. *J. Org. Chem.* **1990**, *55*, 5714.
(5) Lehn, J. M.; Ziessel, R. *Helv. Chim. Acta* **1988**, *71*, 1511−1516.
(6) Scott, J. D.; Puddephatt, R. J. *Organometallics* **1983**, *2*, 1643.

10.1021/ic020430l CCC: $22.00
Published on Web 11/16/2002

were recorded on an Inova 700 spectrometer (^{1}H 400 MHz, ^{13}C 100.6 MHz). NMR chemical shifts are reported in ppm and referenced to residual solvent resonance peaks. High-resolution mass spectra were obtained on a Kratos MS80 RFAQQ instrument.

[2.1.1]-(2,6)-Pyridinophane, $C_{19}H_{17}N_3$, 3. A flame-dried 300-mL Schlenk flask equipped with a Teflon valve and connected to a vacuum-argon line was filled with purified argon. In the flask 50 mL of diethyl ether was added. Then 2,6-lutidine (23.5 mL, 0.20 mol) distilled over calcium hydride under argon atmosphere was introduced. The flask was then placed into an ice bath, and *n*-butyllithium solution in hexane (20.0 mL of 10 M, 0.20 mol) was added dropwise with stirring. After the addition of *n*-butyllithium was complete, the flask with the dark red solution was removed from a bath and left at ambient temperature for 1 h. Diethyl ether was removed in a vacuum, and the yellow crystalline residue was dried at 0.1 Torr during 1 h. Then 1,2-bis(2-pyridyl)ethane (9.20 g, 0.050 mol) dissolved in toluene (50 mL) was added. The flask was immersed for 24 h into a silicon oil bath heated to 170 °C. The initially yellowish-black mixture finally turned dark red. Then the reaction mixture was cooled, and methanol (16 mL) was added to decompose lithium hydride. After the addition of water (18 mL), a yellowish-brown liquid could be easily separated by filtration from a white precipitate of lithium hydroxide. The liquid was dried over solid potassium hydroxide and fractionally distilled first at ambient pressure to recover lutidine and then under vacuum. Yield of crude [2.1.1]-(2,6)-pyridinophane: 7.0 g (50%). bp 190−200 °C at 0.2 Torr. After complete solidification the crude product was recrystallized from heptane three times. Colorless prisms (3.5 g), mp 142−143 °C. ^{1}H NMR ($CDCl_3$, 25 °C, δ): 3.17 (s, 4H, C_2H_4), 4.11 (s, 4H, CH_2), 6.85 (d, J = 7.6 Hz, 2H, *m*-CH_C), 6.96 (d, J = 7.6 Hz, 2H, *m*-CH), 6.97 (d, J = 7.6 Hz, 2H, *m*-CH), 7.39 (t, J = 7.6 Hz, 2H, *p*-CH), 7.43 (t, J = 7.6 Hz, 1H, *p*-CH_C). ^{13}C NMR (CD_2Cl_2, −40 °C, δ): 39.09 (C_2H_4), 45.64 (CH_2), 119.97, 120.62, 120.77 (*m*-C), 136.29 (C4), 136.36 (*p*-C_C), 158.27, 158.87, 160.82 (*o*-C). High-resolution mass spectrum, *m*/*z*: found 287.14128, calcd 287.14225, $C_{19}H_{17}N_3$. Anal. Calcd for $C_{19}H_{17}N_3$: C, 79.4; H, 5.96; N, 14.6. Found: C, 79.3; H, 5.98; N, 14.5.

9,9,16,16-Tetramethyl-[2.1.1]-(2,6)-pyridinophane (tetramethyl-[2.1.1]-(2,6)-pyridinophane), $C_{23}H_{25}N_3$, 2. (a) 2,6-Bis(6-methyl-2-pyridylmethyl)pyridine (6,6″-dimethyltripyridinedimethane),[7] $C_{19}H_{19}N_3$. A flame-dried 300-mL Schlenk flask equipped with a Kontes Teflon valve connected to a vacuum-argon line was charged with 50 mL of diethyl ether and 2,6-lutidine (23.3 mL, 0.20 mol; distilled from calcium hydride). The flask was then cooled to 0 °C, and *n*-butyllithium solution in hexane (20.0 mL of 10 M, 0.2 mol) was added dropwise with stirring. After the addition of *n*-butyllithium was complete, the dark red solution was permitted to warm to ambient temperature for 1 h. Diethyl ether was removed in a vacuum, and the yellow residue was dried at 0.1 Torr for 1 h. Toluene (50 mL) was added via cannula, and 2-picoline distilled over calcium hydride under argon atmosphere (9.9 mL, 0.1 mmol) was added with a syringe. The flask was then immersed for 40 min into a silicon oil bath heated to 120 °C to distill off residual ether and to evolve dihydrogen. Usually 10−20 mL of a liquid was collected. Then the Teflon valve was closed, and the temperature of the silicon oil bath was raised to 145 °C. At the end of the synthesis (12 h) the reaction mixture turned purple-red. Then the reaction mixture was cooled, and methanol (16 mL) was added with a syringe to decompose precipitated lithium hydride. After the addition of water (18 mL), a yellow liquid could be easily separated by filtration from the white precipitate of lithium hydroxide. The liquid was dried over solid potassium hydroxide and fractionally distilled, first at ambient pressure and then under vacuum. Yield of crude 6,6″-dimethyltripyridinedimethane: 12 g (80%). Recrystallization from hexanes yields white crystals: 10 g (70%). mp 68−68.5 °C. bp 173−178 °C at 0.15 Torr. ^{1}H NMR (25 °C, $CDCl_3$, δ): 2.51 (s, 6H, CH_3), 4.29 (s, 4H, CH_2), 6.95 (d, J = 7.5 Hz, 2H, C5terminal-H), 6.96 (d, J = 7.5 Hz, 2H, C3terminal-H), 6.99 (d, J = 7.2 Hz, 2H, C(3,5)central-H), 7.42 (t, J = 7.5 Hz, 2H, C4terminal-H), 7.45 (t, J = 7.2 Hz, 1H, C4central-H). ^{13}C NMR ($CDCl_3$, 20 °C, δ): 24.73 (CH_3), 47.49 (CH_2), 120.66, 121.06, 121.24 (C(3,5)), 136.81 (C4terminal), 137.12 (C4central), 158.00, 159.08, 159.29 (C(2,6)). High-resolution mass spectrum, *m*/*z*: found 289.15664, calcd 289.15790, $C_{19}H_{19}N_3$. Anal. Calcd for $C_{19}H_{19}N_3$: C, 78.9; H, 6.62; N, 14.5. Found: C, 78.9; H, 6.58; N, 14.3.

(b) 2,6-Bis[2-(6-methyl-2-pyridyl)-2-propyl]pyridine (6,6″-dimethyltripyridinedipropane), $C_{23}H_{27}N_3$. To a flame-dried 300-mL Schlenk flask equipped with magnetic stirring bar and filled with dry argon was added 6,6″-dimethyltripyridinedimethane (14.5 g, 0.050 mol) and glyme (100 mL). The flask was then placed into an ice bath, and *n*-butyllithium solution in hexane (10.0 mL of 10 M, 0.10 mol) was added dropwise with stirring. After the addition of *n*-butyllithium was complete, the flask with dark red solution was left to stand for 1 h. Then methyl iodide (6.4 mL, 0.10 mol) in glyme (10 mL) was added dropwise with cooling and intensive stirring over the course of 30 min. At the end of the addition the reaction mixture decolorized almost completely. Then another portion of *n*-butyllithium solution in hexane (10.0 mL of 10 M, 0.10 mol) was added to the reaction mixture. Again, methyl iodide (6.4 mL, 0.10 mol) in glyme (10 mL) was added dropwise with cooling and intensive stirring. In 30 min a saturated aqueous solution of potassium hydroxide (25 g) was added with intensive stirring to precipitate dissolved lithium salts. The resulting yellowish liquid was decanted, dried over solid potassium hydroxide, and fractionally distilled first at ambient pressure to recover glyme and then under vacuum. Yield of pure 6,6″-dimethyltripyridinedipropane: 17 g (98%), bp 165−170 °C at 0.13 Torr. ^{1}H NMR ($CDCl_3$, 25 °C, δ): 1.75 (s, 12H, CH_3), 2.50 (s, 6H, CH_3), 6.89 (virtually d, 4H, J = 7.8 Hz, C(3,5)terminal-H), 6.87 (d, J = 7.8 Hz, 2H, C(3,5)central-H), 7.36 (t, J = 7.8 Hz, 2H, C4terminal-H), 7.37 (t, J = 7.8 Hz, 1H, C4central-H). High-resolution mass spectrum, *m*/*z*: found 345.22131, calcd 345.22049, $C_{23}H_{27}N_3$.

(c) 9,9,16,16-Tetramethyl-[2.1.1]-(2,6)-pyridinophane (tetramethyl-[2.1.1]-(2,6)-pyridinophane), $C_{23}H_{25}N_3$, 2. To a flame-dried 300-mL Schlenk flask equipped with magnetic stirring bar and filled with dry argon was added 6,6″-dimethyltripyridinedipropane (11.1 g, 33 mmol) and glyme (200 mL). The flask was cooled then to −10 °C in an acetone−liquid nitrogen bath, and a *n*-butyllithium solution in hexane (6.6 mL of 10 M, 66 mmol) was added dropwise with stirring. After the addition of *n*-butyllithium was complete, the resulting dark red solution was stirred at −10 °C for 1 h. Then the reaction mixture was cooled to −50 °C, and copper(I) iodide (12.6 g, 66 mmol) was added with stirring during 5 min. After 30 min of stirring at −50 °C the mixture was allowed to warm slowly to room temperature and then heated at reflux for 1 h. Precipitation of metallic copper was observed, and the solution decolorized. After being cooled, a saturated aqueous solution of potassium hydroxide (8 g) was added to the mixture with intensive stirring to precipitate dissolved lithium salts. The resulting brown liquid was decanted, dried over solid potassium hydroxide, and fractionally distilled first at ambient pressure and then under vacuum. Yield of crude tetramethyl-[2.1.1]-(2,6)-pyridinophane: 3.5 g (30%), bp 170−175 °C at 0.12 Torr. After complete solidification

(7) Vedernikov, A. N.; Miftakhov, R.; Borisoglebski, S. V.; Caulton, K. G.; Solomonov, B. N. *Chem. Heterocycl. Comp.* **2002**, *418*, 471.

the crude product was recrystallized from heptane. By slow cooling, colorless needles suitable for X-ray analysis were obtained (1.0 g). mp 138−139 °C. ^{1}H NMR ($CDCl_3$, 25 °C, δ): 1.58 (s, 12H, CH_3), 3.04 (s, 4H, CH_2), 6.80 (d, 2H, $J = 7.7$ Hz, *m*-CH), 6.95 (d, $J = 7.7$ Hz, 2H, *m*-CH), 7.13 (d, $J = 7.8$ Hz, 2H, *m*-CH_C), 7.33 (t, $J = 7.7$ Hz, 2H, *p*-CH), 7.54 (t, $J = 7.8$ Hz, 1H, *p*-CH_C). ^{13}C NMR ($CDCl_3$, 20 °C, δ): 27.67 (CH_3), 38.77 (C_2H_4), 47.87 (CMe_2), 115.16, 116.66, 119.82 (*m*-C), 135.54 (*p*-C), 136.06 (*p*-C_C), 159.05, 167.19, 167.51 (*o*-C). High-resolution mass spectrum, *m*/*z*: found 343.20550, calcd 343.20484, $C_{23}H_{25}N_3$. Anal. Calcd for $C_{23}H_{25}N_3$: C, 80.4; H, 7.34; N, 12.2. Found: C, 80.3; H, 7.28; N, 12.1.

Pd(tetramethyl-[2.1.1]-(2,6)-pyridinophane)Cl_2·MeCN, $C_{25}H_{28}Cl_2N_4Pd$. To a dry flask containing a magnetic stirring bar $PdCl_2$ (49 mg, 0.28 mmol) and 10 mL of dry acetonitrile were added. The mixture was heated with stirring under reflux during 1 h until dissolution of solid dichloropalladium(II) was complete. Then tetramethyl-[2.1.1]-(2,6)-pyridinophane (107 mg, 0.31 mmol) dissolved in 5.0 mL of acetonitrile was added to the ice-cooled solution of the dichloropalladium(II) acetonitrile complex. The color of the solution immediately turned from pale orange to red. The resulting solution was reduced in volume to one-third and cooled in a refrigerator at −18 °C overnight. Large red needles suitable for X-ray analysis were filtered off and washed with a small portion of acetonitrile. Yield: 120 mg (83%). Anal. Calcd for $C_{25}H_{28}Cl_2N_4Pd$: C, 53.4; H, 5.02; N, 9.97. Found: C, 53.3; H, 4.98; N, 9.87. ^{1}H NMR (25 °C, $CDCl_3$, δ): 1.81 (s, 6H, *exo*-CH_3), 1.98 (s, 3H, MeCN), 2.09 (s, 6H, *endo*-CH_3), 3.58−3.66 (m, 2H, *exo*-CH), 5.18−5.33 (m, 2H, *endo*-CH), 7.06 (dd, $J = 7.8$ Hz, 1.1 Hz, 2H, *m*-CH), 7.39 (dd, $J = 7.8$ Hz, 1.1 Hz, 2H, *m*-CH), 7.68 (d, $J = 8.0$ Hz, 2H, *m*-CH_C), 7.52 (t, $J = 7.8$ Hz, 2H, *p*-CH), 8.07 (t, $J = 8.0$ Hz, 1H, *p*-CH_C). ^{13}C NMR ($CDCl_3$, 20 °C, δ): 30.27, 33.35 (CH_3), 37.85 (C_2H_4), 50.51 (CMe_2), 120.08, 121.75, 123.43 (*m*-C), 138.70 (*p*-C), 139.36 (*p*-C_C), 161.37, 164.09, 170.25 (*o*-C).

Pd([2.1.1]-(2,6)-pyridinophane)Cl_2, $C_{19}H_{17}Cl_2N_3Pd$. To a dry flask containing a magnetic stirring bar $PdCl_2$ (177 mg, 1.00 mmol) and 20 mL of dry acetonitrile were added. The mixture was heated with stirring under reflux during 1 h until dissolution of dichloropalladium(II) precipitate was complete. Then [2.1.1]-(2,6)-pyridinophane (313 mg, 1.10 mmol) dissolved in 5.0 mL of acetonitrile was added to the ice-cooled solution of the dichloropalladium(II) acetonitrile complex. The color of the mixture remained almost unchanged. The resulting solution was reduced in volume to one-half and cooled in a refrigerator at −18 °C overnight. The reddish-yellow crystalline powder was filtered off and washed with a small portion of acetonitrile. Yield: 440 mg (95%). Anal. Calcd for $C_{19}H_{17}Cl_2N_3Pd$: C, 49.1; H, 3.69; N, 9.04. Found: C, 49.9; H, 3.30; N, 9.20. ^{1}H NMR (−50 °C, CD_2Cl_2): 3.01−3.17 (m, 1H, C_2H_4), 3.23−3.36 (m, 1H, C_2H_4), 3.63−3.77 (m, 1H, C_2H_4), 4.17 (d, $J = 12.8$ Hz, 1H, CH_2), 4.53 (d, $J = 14.8$ Hz, 1H, C′H_2), 5.33−5.45 (m, 1H, C_2H_4), 5.94 (d, $J = 12.8$ Hz, 1H, CH_2), 6.52 (d, $J = 14.8$ Hz, 1H, C′H_2), 6.95 (d, $J = 7.7$ Hz, 1H, *m*-CH), 7.03 (d, $J = 7.7$ Hz, 1H, *m*-CH), 7.25 (d, $J = 7.7$ Hz, 1H, *m*-CH), 7.28 (d, $J = 7.7$ Hz, 2H, *m*-CH_C), 7.36 (d, $J = 7.7$ Hz, 1H, *m*-CH), 7.43 (t, $J = 7.7$ Hz, 1H, *p*-CH), 7.64 (t, $J = 7.7$ Hz, 1H, *p*-CH), 7.67 (t, $J = 7.7$ Hz, 1H, *p*-CH_C).

Pt([2.1.1]-(2,6)-pyridinophane)Me_2, $C_{21}H_{23}N_3Pt$. In a glovebox filled with purified argon a dry flask containing a magnetic stirring bar was charged with $Pt_2Me_4(SMe_2)_2$ (8.0 mg, 28 μmol) dissolved in 0.50 mL of tetrahydrofuran and with [2.1.1]-(2,6)-pyridinophane (8.4 mg, 29 μmol) dissolved in 0.5 mL of tetrahydrofuran. The mixture was left standing overnight. Orange crystals suitable for X-ray analysis were filtered off and washed with several drops of tetrahydrofuran. Yield: 7 mg (50%). Additional compound (up to 95%) can be obtained from the supernatant solution. Anal. Calcd for $C_{21}H_{23}N_3Pt$: C, 49.2; H, 4.52; N, 8.20. Found: C, 49.5; H, 4.52; N, 8.21. ^{1}H NMR (−47 °C, THF-d_8, δ): 0.54 (s, $^2J_{Pt-H} = 89.4$ Hz, 3H, Me), 0.55 (s, $^2J_{Pt-H} = 89.4$ Hz, 3H, Me), 2.85−3.10 (m, 2H, C_2H_4), 3.35−3.49 (m, 1H, C_2H_4), 3.97 (d, $J = 11.3$ Hz, 1H, CH_2), 4.16 (d, $J = 12.6$ Hz, $J_{Pt-H} = 9$ Hz, 1H, CH_2), 5.44−5.58 (m, 1H, C_2H_4), 5.54 (d, $J = 11.3$ Hz, 1H, CH_2), 5.87 (d, $J = 12.6$ Hz, $J_{Pt-H} = 15$ Hz, 1H, CH_2), 6.70 (d, $J = 7.6$ Hz, 1H, *m*-CH), 6.94 (d, $J = 7.6$ Hz, 1H, *m*-CH), 7.15 (d, $J = 7.6$ Hz, 1H, *m*-CH), 7.25 (d, $J = 7.6$ Hz, 1H, *m*-CH), 7.32 (d, $J = 7.6$ Hz, 1H, *m*-CH_C), 7.35 (d, $J = 7.7$ Hz, 1H, *m*-CH_C), 7.29 (t, $J = 7.6$ Hz, 1H, *p*-CH), 7.59 (t, $J = 7.7$ Hz, 1H, *p*-CH), 7.64 (t, $J = 7.6$ Hz, 1H, *p*-CH_C). ^{13}C NMR (CD_2Cl_2, −40 °C, δ): −24.75 (s, $J_{Pt-C} = 845$ Hz), −24.43 (s, $J_{Pt-C} = 845$ Hz) (CH_3), 33.45, 37.73 (C_2H_4), 47.19, 47.33 (CH_2), 120.08, 121.04, 121.90, 122.07, 123.30, 123.41 (*m*-C), 136.30, 136.67, 136.94 (*p*-C), 155.00, 157.13, 157.16, 158.24, 160.43, 164.45 (*o*-C).

Crystal Structure of (2)$PdCl_2$·MeCN. A nearly equidimensional fragment sample was cleaved from a larger transparent orange needle. The selected fragment was then affixed to a glass fiber using silicone grease and transferred to the Bruker SMART6000 CCD system where it was cooled to −160 °C using a gas-flow cooling system of local design. A set of initial frames indicated that the crystal was single. The data were collected using 10-s frames with an ω scan of 0.30°. Data were corrected for Lorentz and polarization effects, and equivalent reflections were averaged using the Bruker SAINT software as well as utility programs from the XTEL library. The structure was solved using SHELXTL and Fourier techniques. Systematic absences and statistical tests indicated the noncentrosymmetric space group *Pnma* with $Z = 4$. The solution and refinement confirmed this assignment, and the molecule lies on a mirror plane. A solvent molecule (MeCN) was also present, also lying on a mirror plane. All of the hydrogen atoms were clearly visible in a difference Fourier and were refined isotropically in the final cycles of refinement, with the exception of the three hydrogen atoms associated with the MeCN solvent. The latter were disordered over two positions and were placed in fixed positions with 50% occupancy. All structural parameters are within normally accepted values. A final difference Fourier was essentially featureless, with all peaks being less than 0.46 e/Å^3.

X-ray Structure Determination of $C_{23}H_{25}N_3$, 2. A suitable sample was cleaved from a larger transparent needle. The selected fragment was then affixed to a glass fiber using silicone grease and transferred to the Bruker SMART 6000 CCD system where it was cooled to −160 °C using a gas-flow cooling system of local design. A set of initial frames indicated that the crystal was single. The data were collected using 60-s frames with an ω scan of 0.30°. Data were corrected for Lorentz and polarization effects, and equivalent reflections were averaged using the Bruker SAINT software as well as utility programs from the XTEL library. The structure was solved using SHELXTL and Fourier techniques. Systematic absences and statistical tests indicated the noncentrosymmetric space group $P2_12_12_1$ with one unique molecule. The solution and refinement confirmed this assignment. All of the hydrogen atoms were clearly visible in a difference Fourier and were refined isotropically in the final cycles of refinement. A final difference Fourier was essentially featureless, with all peaks being less than 0.16 e/Å^3.

Computations. Theoretical calculations in this work have been performed using density functional theory (DFT) method,[8] specif-

(8) Parr, R. G.; Yang, W. *Density-functional Theory of Atoms and Molecules*; Oxford University Press: Oxford, 1989.

Scheme 1

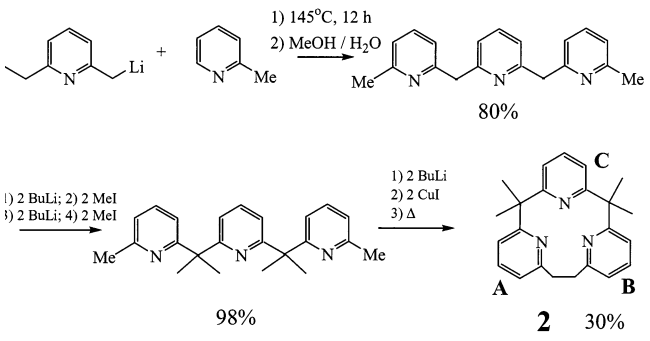

ically functional PBE,[9] implemented in an original program package Priroda.[10] In PBE calculations, relativistic Stevens−Basch−Krauss (SBK) effective core potentials (ECP)[11] optimized for DFT calculations have been used. The basis set was a 311-split for main group elements with one additional polarization *p*-function for hydrogen, and an additional two polarization *d*-functions for elements of higher periods. Full geometry optimization was performed without constraints on symmetry. For all species under investigation, frequency analysis has been carried out. All minima have been checked for the absence of imaginary frequencies. Reaction trajectories have been calculated by the method of Gonzales and Schlegel.[12]

Results

Synthesis and Characterization of Pyridinophane 2 and its $PdCl_2$ Complex. Pyridinophane **2** is synthesized by the path shown in Scheme 1. Its structure is best deduced by ^{1}H NMR spectroscopy and shows mirror symmetry. Four equivalent methyl groups indicate only a small barrier for conformational reorientation of one of the rings to the opposite side of the three-nitrogen plane. A crystal structure determination (Figure 1a) shows a conformation where the A and B ring lone pairs point in opposite directions.

Reaction of **2** with $PdCl_2(NCMe)_2$ at 25 °C in acetonitrile, followed by overnight cooling at −18 °C, gives pure crystalline (**2**)$PdCl_2$ containing MeCN in the lattice, whose ^{1}H NMR spectrum shows mirror symmetry relating the A and B rings. In contrast to the free ligand **2**, complex (**2**)$PdCl_2$ exhibits two unequivalent CMe_2 methyl proton chemical shifts because of a rigid mirror symmetric structure resulting from binding to $PdCl_2$. Protons of the $(CH_2)_2$ bridge resonate as an AA′XX′ system, consistent with the conclusion on rigidity of the molecule.

The X-ray diffraction structure of the molecule (Figure 1b) shows a rigorous mirror symmetric *cis*-$PdCl_2$ group bound to the A and B rings of **2** in a conventional fashion. Such binding indeed brings the C ring in proximity to Pd, but the near-planar $Pd(N)_2Cl_2$ substructure leaves the d_{z^2} orbital doubly occupied, so the out-of-plane coordination sites

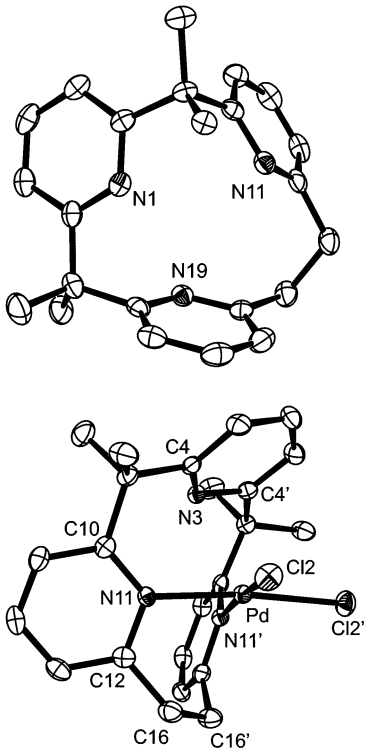

Figure 1. (a) ORTEP drawing of the non-hydrogen atoms of pyridinophane **2**. Unlabeled atoms are carbon. Thermal ellipsoids are given at 50% level of probability. (b) ORTEP drawing of the non-hydrogen atoms of (**2**)$PdCl_2$. Unlabeled atoms are carbon. Selected bond lengths and angles: Pd−Cl(2) = 2.295(1), Pd−N(11) = 2.083(3), N(11)−Pd−N(11′) = 88.53(15)°, Cl(2)−Pd−Cl(2′) = 91.57(5). Thermal ellipsoids are given at 50% level of probability.

around Pd contain electron density; the only empty orbital, $d_{x^2-y^2}$, lies along the Pd−Cl axes. As a result, the ring C nitrogen orients its lone pair away from Pd. The ring constraints in **2** nevertheless leave the face of the C ring, and more specifically leave N and the two ortho carbons located above the $PdCl_2$ plane. There is, therefore, a d_{z^2}/π-cloud repulsion, with Pd/N3 and Pd−C4 separations of 2.658 and 2.944 Å. These are sub-van der Waals contacts, but repulsive. For comparison, the distances from Pd to C16 and its *syn* H are 2.938 and 2.765 Å. There is evidence of a minor deformation of Pd out of the N11N11′ Cl2 and Cl2′ plane (the Pd atom deviates from the plane by 0.14 Å toward the ring C) to rehybridize the d orbitals and diminish the pure $(d_{z^2})^2$ character of the repulsion. Spectroscopic evidence for this unusual Pd/C ring interaction is found in the ^{1}H NMR chemical shifts. The C ring meta and para chemical shift changes on (**2**)$PdCl_2$ (vs their values in free **2**) are larger (by 0.58 and 0.53 ppm) than are the changes for protons of the two other rings.

We investigated experimentally the possibility that these Pd/N (ring C) repulsions might be diminished in the unsymmetrical isomer because DFT calculations (PBE[9] functional, program package Priroda[10]) show the out-of-plane Pd/N distance to be longer (3.33 Å) there than calculated in the symmetrical isomer (2.81 Å). This longer distance in the unsymmetrical isomer originates from the longer tether (C_2H_4) to the pendant pyridyl ring. However, we observed no isomerization (eq 1) of *sym*-(**2**)$PdCl_2$ into its unsym-

(9) Perdew, J. P.; Burke, K.; Ernzerhof, M. *Phys. Rev. Lett.* **1996**, *77*, 3865.
(10) (a) Usytnyuk, Y. A.; Ustynyuk, L. Y.; Laikov, D. N.; Lunin, V. V. *J. Organomet. Chem.* **2000**, *597*, 182. (b) Laikov, D. N. *Chem. Phys. Lett.* **1997**, *281*, 151.
(11) (a) Stevens, W. J.; Basch, H.; Krauss, M. *J. Chem. Phys.* **1984**, *81*, 6026. (b) Stevens, W. J.; Basch, H.; Krauss, M.; Jasien, P. *Can. J. Chem.* **1992**, *70*, 612. (c) Cundari, T. R.; Stevens, W. J. *J. Chem. Phys.* **1993**, *98*, 5555.
(12) Gonzales, C.; Schlegel, H. B. *J. Phys. Chem.* **1991**, *95*, 5853.

Scheme 2

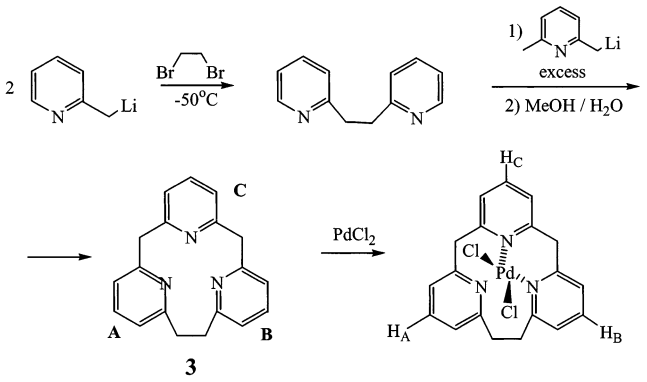

metrical isomer with the palladium bound to nitrogens of unequivalent pyridine rings B and C: heating a solution of *sym*-(**2**)$PdCl_2$ in acetonitrile to 60 °C does not lead to either any line broadening (^{1}H NMR at 60 °C) or appearance of new set of signals.

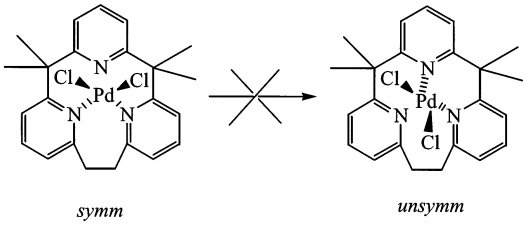

(1)

This is consistent with the result of DFT calculations (PBE functional) that $\Delta G°_{298} = 3.0$ kcal/mol in favor of the symmetrical isomer. According to the calculated structure of *uns*-(**2**)$PdCl_2$, one of the CH_3- groups is very close to the Pd atom so forcing a Pd−H distance of 2.33 Å. Thus, the weaker interactions of some of the *gem*-dimethyl groups with Cl on Pd seem to determine the isomer preference.

Synthesis and Characterization of the Nonmethylated Pyridinophane 3 and Its $PdCl_2$ and $PtMe_2$ Complexes. If the four methyl groups at the bridging carbons of the macrocycle **2** affect significantly its preferred binding modes, the nonmethylated [2.1.1]-(2,6)-pyridinophane **3** ($n = 2$) should show properties significantly different from those of the macrocycle **2**. We synthesized [2.1.1]-pyridinophane in two steps with a total yield of 40% according to Scheme 2.

The dichloropalladium(II) complex of pyridinophane **3**, (**3**)$PdCl_2$, is formed at 20 °C in acetonitrile from dichloropalladium(II). (**3**)$PdCl_2$ exhibits fluxional behavior at room temperature in CD_2Cl_2 solution because of rapid palladium atom migration between nitrogens of the A and B rings of the ligand **3**. The only sharp signal in its ^{1}H NMR spectrum corresponds to H−C (para) of the ligand **3** central pyridine ring (Scheme 2). Signals of other ligand protons appear as broad singlets with the exception of H−C (meta) of the **C** ring, which shows one broadened doublet at room temperature. The broadened singlets become resolved as multiplets at −35 °C, characteristic of a molecule with no symmetry. Resolved are three triplets of H−C (para), six doublets of H−C (meta), and two sets of AX patterns of CH_2- bridges. Thus, and in contrast to (**2**)$PdCl_2$, (**3**)$PdCl_2$ is the unsymmetrical isomer shown in Scheme 2.

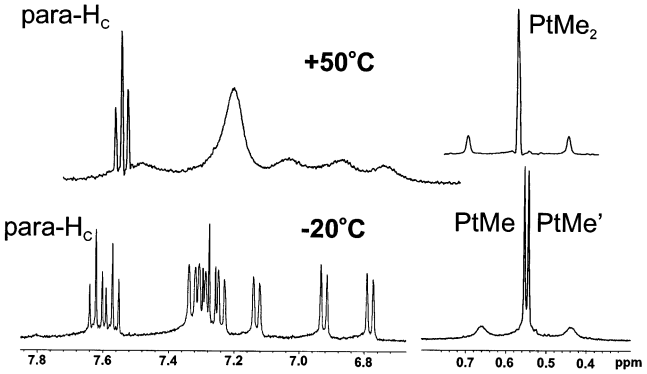

Figure 2. ^{1}H NMR spectra of (**3**)$PtMe_2$ in tetrahydrofuran-d_8 at various temperatures.

The experimental preference for *uns*-(**3**)$PdCl_2$ over its symmetrical isomer is in agreement with results of DFT calculations, which show that *uns*-(**3**)$PdCl_2$ is favored over its symmetrical isomer by $\Delta H°_{298} = 5.6$ kcal/mol. The main cause of this may be lower repulsive interactions between the filled metal d_{z^2} orbital and the central pyridine ring π-electrons (or electrons of the nitrogen lone pair) in the former (palladium−nitrogen distance of 3.14 versus 2.71 Å in the symmetrical isomer, again because of the longer tether to the pendant pyridyl group), without significant intervention of $PdCl_2$ interactions with hydrogens of the CH_2- bridges, in contrast to the complex derived from the ligand **2**.

Mechanism of Fluxional Rearrangement. This rearrangement might occur with (eq 2a), or without (eq 2b), site exchange of the chloride ligands. In principle, we cannot exclude also existence of an equilibrium between **4a** and **4b**. The difference hinges on whether the $PdCl_2$ plane lies in (eq 2b) or perpendicular to (eq 2a) the mirror plane present at the transition state (or intermediate) of the mechanism. To establish this mechanistic feature we undertook both experimental and DFT investigations. An analogue with NMR-active methyl groups in place of chlorides was synthesized by reaction of **3** with $Pt_2Me_4(\mu\text{-}SMe_2)_2$. Use of Pt rather than Pd permits use of spin coupling to test for unimolecular character in the mechanism. Proton NMR

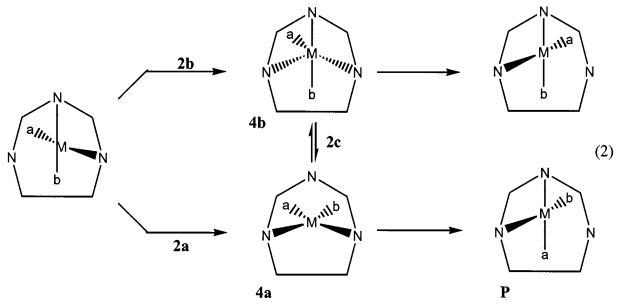

spectroscopy (Figure 2) shows that (**3**)$PtMe_2$ adopts the unsymmetrical structure (three triplets of H−C (para), six doublets of H−C (meta), and two sets of AX patterns for the CH_2- bridges at −20 °C) and is fluxional, analogous to (**3**)$PdCl_2$. At 20 °C in THF-d_8,[13] all protons except the H−C (para) of the central ring are broad multiplets, and the methyl groups appear as one broadened singlet but with discernible

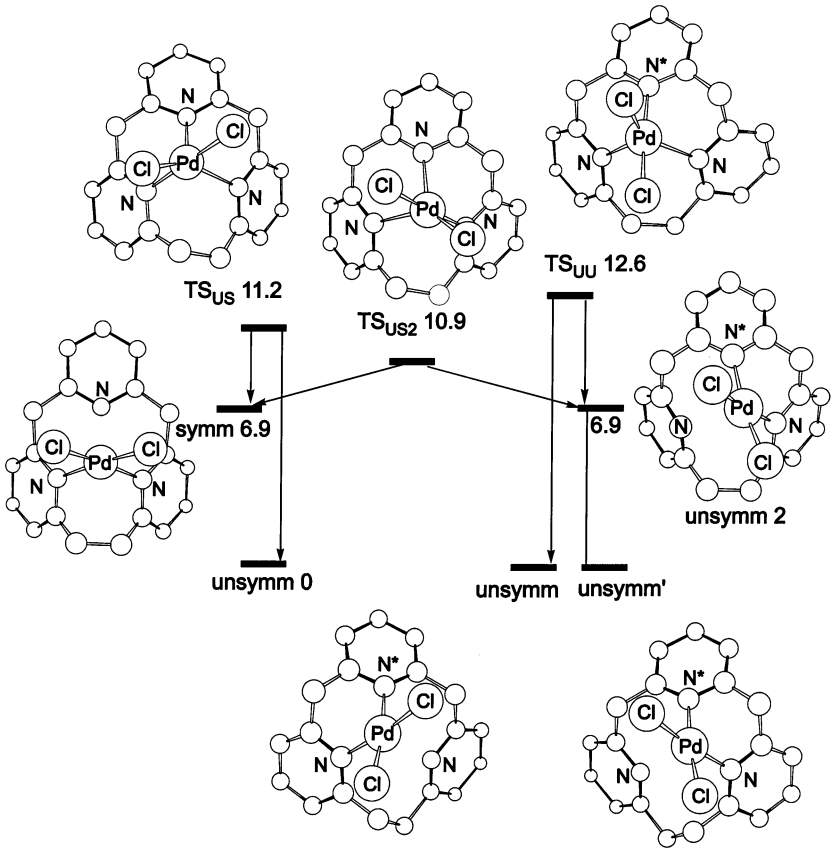

Figure 3. DFT free energies (298 K, kcal/mol) and structures for species involved in isomerization and enantiomerization of (**3**)$PdCl_2$.

platinum satellites ($^2J_{Pt-H}$ = 90 Hz). At +50 °C, signals of some of the C_2H_4 group protons have sharpened somewhat. At −5 °C, the methyl groups have decoalesced into two sharp singlets ($^2J_{Pt-H}$ = 89 Hz for each). At −47 °C, all protons of all pyridine rings are as sharp as that of H−C (para) of the central ring of **3**. At this temperature protons of one of the CH_2- bridges show significant coupling with ^{195}Pt (15 and 12 Hz) indicating proximity of one of the bridges to the metal atom. The fluxional process for the $PtMe_2$ derivative thus has a higher activation energy than does the $PdCl_2$ analogue, and the pyridine ring exchange mechanism clearly involves site exchange of the unequivalent methyl ligands (eq 2). The midpoint of this rearrangement thus involves the isomeric structure, which is the ground state for (**2**)$PdCl_2$. The nature of this experimental study can establish the occurrence of mechanism 2a. It cannot, however, confirm or deny the energetic accessibility of mechanism 2b or some mixed mechanism involving high-energy five-coordinate intermediates linking **4a** and **4b** via mechanism 2c. For this, it is necessary to turn to a computational method.

DFT Study of the Mechanism of Fluxionality. For unsymmetrical isomers (**3**)MX_2, the (+) or (−) gauche conformation of C1−C2 bridges of the macrocycle are reversed in the course of their enantiomerization. When the barrier of such conformational transition is high enough, a new isomer of (**3**)MX_2 can appear. Study of the reaction paths of isomerizations 2a and 2b (Figures 3 and 4; paths that have been traced to a given structure are indicated with arrows) showed that it is indeed the case; it revealed the following:

(1) For (**3**)MX_2 complexes (MX_2 = $PdCl_2$ and $PtMe_2$), enantiomers of the unsymmetrical and related symmetrical isomer (intermediate **4a**) can rearrange by passage through two mirror transition states TS_{US} (reaction path 2a). In agreement with experiment, the unsymmetrical isomer is more stable, and relative rates are calculated to be faster for the $PdCl_2$ case (barriers are smaller by 4.2−5.0 kcal/mol).

(2) In the case (Figure 4) of (**3**)$PtMe_2$, two enantiomers of unsymmetrical (**3**)$PtMe_2$ interconvert through the transition state TS_{UU} (isomerization path 2b).

(3) In the case of (**3**)$PtMe_2$, a second distinct path 2a has been found. It connects the enantiomeric *uns*-(**3**)$PtMe_2$ complexes with *sym*-(**3**)$PtMe_2$ via transition state TS_{US2} whose energy is only slightly higher than that of TS_{US}. In contrast to TS_{US}, the formation of TS_{US2} is accompanied by rotation about the C1−C2 bond in another direction.

(4) In the case of (**3**)$PdCl_2$ only, isomerization path 2b includes an additional unsymmetrical intermediate involving rotation about the C1−C2 bond of the macrocycle **3** and some shortening of the Pd−N distance (to 2.763 Å) in this isomer. This *uns*-**2** is an unsymmetrical analogue of (**2**)$PdCl_2$, but in contrast to the latter, the third nitrogen atom here points its lone pair toward the metal. In contrast to (**3**)$PtMe_2$, the unsymmetrical intermediate is stabilized, presumably because

(13) Because of the slower rate versus (**3**)$PdCl_2$, it was necessary to employ THF rather than CD_2Cl_2 to reach the coalescence temperature. At lower temperatures, ^{1}H NMR spectra in CD_2Cl_2 and THF-d_8 were wholly analogous.

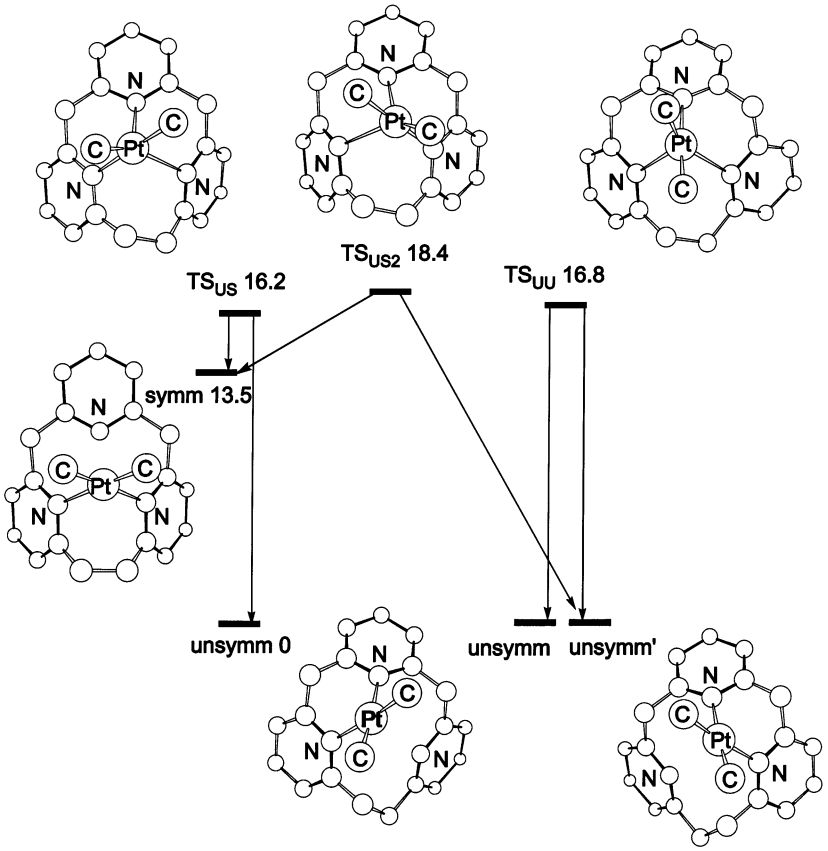

Figure 4. DFT free energies (298 K, kcal/mol) and structures for species involved in isomerization and enantiomerization of (**3**)$PtMe_2$.

of less significant repulsive interactions between the pendant nitrogen and the palladium atom, which bears higher Mulliken positive charge in *uns*-(**3**)$PdCl_2$ (+0.705) than does platinum in (**3**)$PtMe_2$ (+0.671). *uns*-**2** is connected to one of the two unsymmetrical enantiomers through transition state TS_{UU}. *uns*-**2** is also connected by reaction path 2c to the symmetrical isomer through transition state TS_{US2} located at practically the same energy level as TS_{US}. Thus, in the case of (**3**)$PdCl_2$, the two paths of isomerization, 2a and 2b, are connected through related symmetrical and unsymmetrical intermediates.

In summary, the DFT study of enantiomerization reaction paths showed that multiple and almost equally probable competitive mechanisms operate concurrently here for both (**3**)$PdCl_2$ and (**3**)$PtMe_2$.

Discussion

In support of our findings, we note that fluxional processes with hydriodotris(pyrazolyl)borate Pd(II) complexes [Tp*Pd(R)(PPh_3)] (R = Me, *p*-Tol, Ac, *p*-TolCO) have been shown by IR spectroscopy to not involve any five-coordinated intermediates but to proceed presumably via five-coordinated transition states.[14] For d^8 Rh(I) hydriodotris(pyrazolyl)borate complexes [$Tp^{Me2,4Cl}$Rh(CO){$P(OR)_3$}] (R = Me, Ph) five-coordinated species have been found both in the solution and in the solid state with one Rh−N distance 0.66 Å longer than the other two.[15,16] Similarly, five-coordinated Rh(I) complexes [Rh(L){bis[(3,5-dimethyl-1-pyrazolyl)methyl]ethylamine}]BF_4 (L = cod, $(CO)_2$) have been found in the solid state (but not in solution) with one Rh−N distance longer by 0.47 Å.[16]

The pyridinophanes may join the current range of facial preference ligands C_5R_5, RE(pyrazolyl)$_3$ (E = N, C, B),[17,18] 3-fold symmetric cyclic triamines[19] and thioethers,[20] and the various tripodal thianes,[21] phosphines,[22] tripyridine methanes,[23] and amides[24,25] in manipulating metal center thermodynamics and reactivity. The present work shows the ability of [2.1.1]-pyridinophanes to adapt to an η^2-mode of binding,

(14) Klaui, W.; Turkowski, B.; Wunderlich, H. Z. *Anorg. Allg. Chem.* **2001**, *627*, 2397.

(15) Malbosc, F.; Chauby, V.; Serra-Le Berre, C.; Etienne, M.; Daran, J. C.; Kalk, P. *Eur. J. Inorg. Chem.* **2001**, 2689.

(16) Mathieu, R.; Esquius, G.; Lugan, N.; Pons, J.; Ros, J. *Eur. J. Inorg. Chem.* **2001**, 2683.

(17) Slugovc, C.; Padilla-Martinez, I.; Sirol, S.; Carmona, E. *Coord. Chem. Rev.* **2001**, *213*, 129.

(18) Tellers, D. M.; Skoog, S. J.; Bergman, R. G.; Gunnoe, T. B.; Harman, W. D. *Organometallics* **2000**, *19*, 2428.

(19) Busch, D. H.; Stephenson, N. A. *Coord. Chem. Rev.* **1990**, *100*, 119.

(20) Blake, A. J.; Gould, R. O.; Li, W.; Lippolis, V.; Parsons, S.; Radek, C.; Schroeder, M. *Inorg. Chem.* **1998**, *37*, 5070.

(21) Schebler, P. J.; Mandimutsira, B. S.; Riordan, C. G.; Liable-Sands, L. M.; Incarvito, C. D.; Rheingold, A. L. *J. Am. Chem. Soc.* **2001**, *123*, 331.

(22) Kyba, E. P.; Davis, R. E.; Hudson, C. W.; John, A. M.; Brown, S. B.; McPhaul, M. J.; Liu, L.-K.; Glover, A. C. *J. Am. Chem. Soc.* **1981**, *103*, 3868.

(23) Canty, A. J.; Fritsche, S. D.; Jin, H.; Honeyman, R. T.; Skelton, B. W.; White, A. H. *J. Organomet. Chem.* **1996**, *510*, 281.

(24) Renner, P.; Galka, C. H.; Gade, L. H.; Radojevic, S.; McPartlin, M. *Eur. J. Inorg. Chem.* **2001**, 1425.

(25) MacBeth, C. E.; Golombek, A. P.; Young, V. G., Jr.; Yang, C.; Kuczera, K.; Hendrich, M. P.; Borovik, A. S. *Science* **2000**, *289*, 938.

a capability of increasing importance in tris-pyrazolylborate chemistry.

The potentially tetradentate macrocycle **5** has attracted attention recently[26−31] as a ligand to many metals. When it

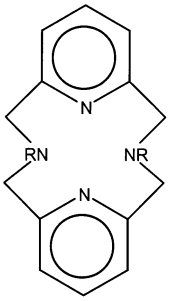

5

does bind η^3, one RN group is pendant, it can enable a site exchange with the coordinated NMe group, and in one instance this nitrogen has been protonated; this last function may be useful in future applications of pyridinophanes requiring proton transfer to complete some substrate conversion.[32]

In summary, the pyridinophanes studied here offer some interesting and geometrically controllable (via ligand methylation) opportunities to investigate the influence of nucleophile/nucleophile repulsions on the reactivity of d^8 metal complexes. The degenerate rearrangement between enantiomers of the unsymmetrical structure involves a transition state that is thermally accessible at 25 °C. We have studied this computationally in considerable detail to establish the energies of flexing this new macrocycle since this will be a component of certain types of its reactivity (e.g., protonation or oxidative addition). This work shows that a MX_2 electrophile (M = Pd, Pt; X = halide, alkyl) finds numerous ways to bind η^2 to [2.1.1]-(2,6) pyridinophane, and all these differ in energy by less than 15 kcal/mol. The presence of a pendant nucleophile poised to bind to the metal may lead to unusual reactivity when these metals are oxidized to M(IV).

Acknowledgment. This work was supported by the Department of Energy. This work has been made possible in part because of support from Russian Foundation for Basic Research (Grant 01.03.32692).

Supporting Information Available: Full crystallographic details for Figure 1. This material is available free of charge via the Internet at http://pubs.acs.org.

IC020430L

(26) Koch, W. O.; Kaiser, J. T.; Kruger, H. *Chem. Commun.* **1997**, 2237.
(27) Koch, W. O.; Barbieri, A.; Grodzicki, M.; Schuenemann, V.; Trautwein, A. X.; Krueger, H. *Angew. Chem., Int. Ed. Engl.* **1996**, *35*, 422.
(28) Kelm, H.; Krueger, H. *Eur. J. Inorg. Chem.* **1996**, 1381.
(29) Kelm, H.; Krueger, H. *Inorg. Chem.* **1196**, *35*, 3533.
(30) Meneghetti, S. P.; Lutz, P. J.; Kress, J. *Organometallics* **2001**, *20*, 5050.
(31) Meneghetti, S. P.; Lutz, P. J.; Fischer, J.; Kress, J. *Polyhedron* **2001**, *20*, 2705.
(32) Casey, C. P.; Singer, S. W.; Powell, D. R.; Hayashi, R. K.; Kavana, M. *J. Am. Chem. Soc.* **2001**, *123*, 1090.